

See discussions, stats, and author profiles for this publication at: <https://www.researchgate.net/publication/221503838>

# Position control of a pneumatic levitation system.

Conference Paper · January 2005

DOI: 10.1109/ETFA.2005.1612568 · Source: DBLP

---

CITATIONS

16

READS

1,935

3 authors, including:



Juan Manuel Escaño

Universidad de Sevilla

69 PUBLICATIONS 216 CITATIONS

[SEE PROFILE](#)



Francisco R. Rubio

Universidad de Sevilla

123 PUBLICATIONS 3,454 CITATIONS

[SEE PROFILE](#)

Some of the authors of this publication are also working on these related projects:



Multi-terminal HVDC Grids Supervisory Control [View project](#)



Control and Optimization of Hybrid DC/AC Power System [View project](#)

# Position Control of a Pneumatic Levitation System

Juan M. Escaño\*, Manuel G. Ortega, and Francisco R. Rubio †

## Abstract

The position control of a pneumatic levitation system is described in this paper. The control system uses visual feedback to compute the object position, which can be modified by means of an air blower acted by a variable-speed drive. The system is employed as a test bed of control strategies. A performance comparison attained by a classical PID, a robust  $H_\infty$  control law and a fuzzy controller is carried out, including tracking and disturbance rejection experiments.

Pneumatic levitation, robust control, fuzzy control, control applications.

## 1 Introduction

The use of pneumatic levitation systems is a not sufficiently exploited application, perhaps because of their difficulty to regulate the vertical movements of the floating objects. Nowadays there exist prototypes of this kind of systems applied, among others, to food carriage (for example, see [8]). The main advantages of this kind of transport are the low friction and the material management without any contact with mechanical parts. Therefore, a too much cleaner and faster conveyance is achieved with this kind of devices.

In this work a lab plant, which consists of industrial components is employed to test several control strategies applied to pneumatic levitation systems. The main goal is to fulfill a real time control on the position of an object (in this case a ball) hovering in a air current, which catches the ball with some force.

The device is located at the Process Control Laboratory of the *Altair Technological Center* in Seville (Spain), which consists of a centrifugal fan blower acted by an AC motor connected to a variable-speed drive. The drive speed-reference is sent from a trading programmable logic controller (PLC), which receives the ball position measurement from a personal computer linked to it through

\*J.M. Escaño is with the Depto. Electricidad y Automática, Centro Tecnológico Altair, Barbero de Sevilla, 1 – 41006 Sevilla, (Spain), email:jmesc@e-altair.org

†M.G. Ortega and F.R. Rubio are with the Depto. Ingeniería de Sistemas y Automática, Escuela Técnica Superior de Ingenieros, Universidad de Sevilla, Camino de los Descubrimientos, s/n – 41092 Sevilla (Spain) email:{mortega,rubio}@esi.us.es

an Ethernet using the MODBUS protocol based on TCP-IP. Finally, the ball position is computed by means of a camera connected to the PC, which has an appropriate image processing software available [1]. Figure 1 shows a scheme of the application and a picture of the system is exposed in figure 2.

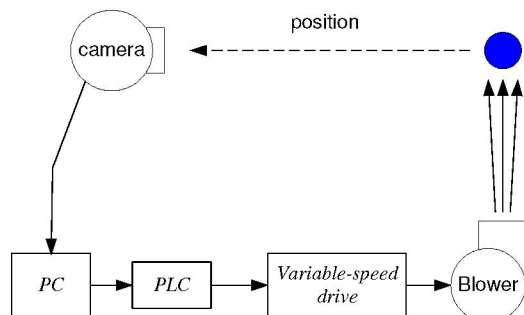


Figure 1. Scheme of the application

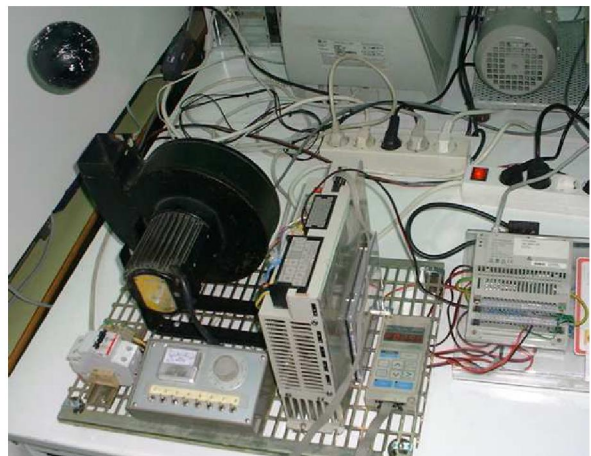
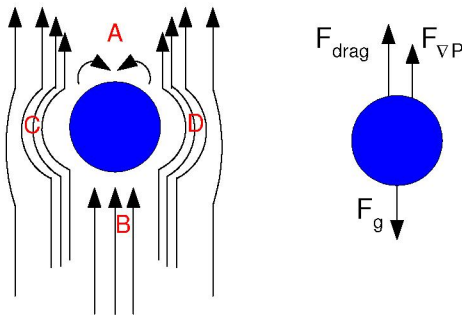


Figure 2. Picture of the system

The remainder of the paper is organized as follows: in Section 2 a brief theoretical study for system modelling is presented, and the results of the system identification at several operating points are exposed. The description of the synthesis of the different controllers, as well as a comparison among the performances achieved, are shown in Section 3. Finally, major conclusions are summarized in Section 4.

## 2 System model

The system behavior can be understood by means of the motion model of a body sunken within the pale of a gaseous stream. Starting from figure 3, a null gas velocity at points A and B can be concluded. Besides, velocity at points C and D is greater than the one at points far from the ball surface. From Bernoulli's equation, it can be stated that high air velocity zones are low pressure and vice versa. Therefore, a pressure difference is produced from the airflow center to the far away zones, which makes the ball almost to maintain its lateral position along the air stream.



**Figure 3. Forces acting on the ball**

A complete model of the system may result quite difficult to obtain. In a simplified manner, it can be stated that the main forces acting on the ball (see figure 3) are:

- *Dragging forces of air resistance:*  $F_{drag} = \frac{C_D}{2} \rho_a \pi r^2 v^2$ , where  $v$  is the air flow velocity,  $\rho_a$  is the air density,  $r$  is the ball radius, and  $C_D$  is the drag coefficient of the object.
- Forces due to *gradients of air pressure:*  $F_{\nabla P} = \frac{2}{3} \pi r^3 \rho_a \frac{dv^2}{dh}$ , where  $h$  is the vertical distance between the ball and the centrifugal fan.
- *Gravity force:*  $F_g = \frac{4}{3} \pi r^3 \rho_b g$ , where  $\rho_b$  is the ball density, and  $g$  is the gravity constant.

Therefore, the resulting vertical net force,  $F_R(h)$ , acting on the ball can be computed as follows:

$$F_R(h) = -F_g + F_{\nabla P} + F_{drag}$$

and by applying the Newton's Second Law, the vertical motion of the ball can be modelled. It is worth pointing out the dependency of the air flow velocity,  $v$ , on the distance to the fan output,  $h$ . Although there exists a wide zone where the velocity can be considered to be proportional to  $h^{-1}$ , if  $h$  is large enough (in this application, about 50 cm) the flow velocity decreases drastically, becoming its dynamics very complex.

From the above equations, and taking into account that other effects (such as lateral and rotational motions, lack

of sphericity, rugosity, etcetera) have not been considered, it is easy to realize that having an accurate model of the object motion results very complicated. Furthermore, the flow velocity at the fan output is modified by means of the variable-speed drive, but no measurement of the velocity is available. This implies that the fan dynamics should be also modelled.

Due to the complexity of the system, some linear models are derived at several operating points in order to synthesize some model-based controller. Thereby, excited enough control signals around three equidistant operating points are supplied. From input-output data analysis, and by using an appropriate software package for example, [6], transfer functions are obtained, whose frequency responses are plotted in figure 4. A nominal model, whose frequency response is also included in figure 4 (thick line), is chosen as follows:

$$G_N(s) = \frac{-0.4023s^4 + 13.97s^3 - 111.8s^2 - 533.3s + 5881}{s^4 + 45.82s^3 + 178.3s^2 + 998s + 2542}$$

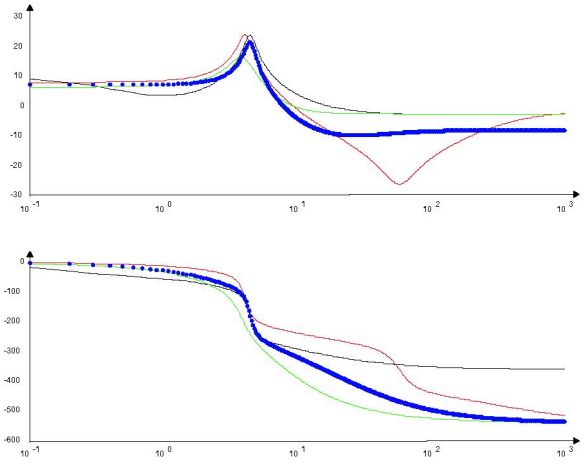


**Figure 4. Frequency responses at several operating points**

It can be checked that the system is stable, with a dominant pair of complex poles, which makes the step response of the system be very oscillatory (see figure 5).

## 3 Control strategies

The following three control strategies has been implemented in this system: a classical PID controller, a robust control law based on the  $H_\infty$  mixed sensitivity approach and a controller based on fuzzy logic.

Two kind of experiments are carried out in order to test the performance supplied by these control strategies: tracking experiments applying a step-change of 20 cm at the position reference, and disturbance rejection experiments, in which some air flow is removed by hand during a small time interval.

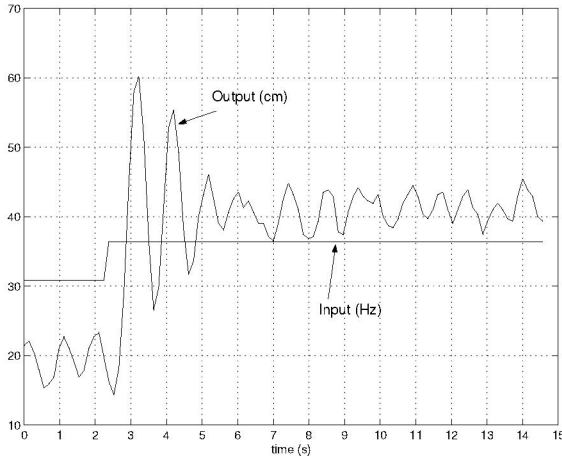


**Figure 5. Step response of the nominal model**

### 3.1 PID control law

The first strategy implemented is based on the classical Proportional-Integral-Derivative controller. A first set of values for its gains is performed by means of the well-known Ziegler-Nichols tuning rules; afterwards a fine adjustment is fulfilled to attain a better behavior.

Figure 6 shows some experimental results obtained with this control strategies. In this case, it can be observed a good tracking response, while the disturbance rejection experiment exhibits a slow and too oscillatory behavior.

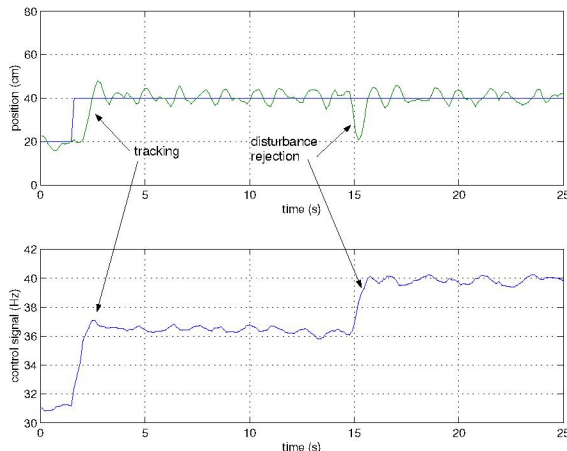


**Figure 6. Experimental results with the PID controller**

### 3.2 $H_\infty$ controller

A robust  $H_\infty$  control law based on the  $S/KS/T$  mixed sensitivity problem [10] has been also tested. With this control strategy, closed-loop sensitivity functions are shaped using some weighting functions. This configuration is shown in figure 7, where  $P(s)$  is the so-called *generalized plant*, and  $\omega$ ,  $z$ ,  $v$  and  $u$  represent the exogenous

signals, the error vector, the measured variable and the control signal respectively.

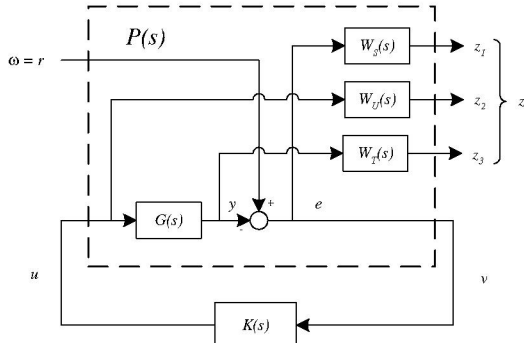


**Figure 7.  $S/KS/T$  mixed sensitivity configuration**

The design of appropriate weighting functions has been carried out by means of the procedure exposed in [7]. Next, steps followed to synthesize the  $H_\infty$  controller are exposed:

1. Scaling and estimation of the multiplicative output uncertainty

At this first step, the identified transfer functions as well as the nominal model selected must be scaled. This is carried out, as stated in [10], using the maximum desired variation of control signal, as well as the maximum allowed variation of the output.

Using these scaled functions, the multiplicative uncertainty with respect to the nominal model is estimated as follows:

$$E_{oi}(s) = (\hat{G}_i^*(s) - \hat{G}_N(s))\hat{G}_N(s)^{-1} \quad i = 1, \dots, p$$

where  $\hat{G}_N(s)$  represents the scaled nominal model and  $\hat{G}_i^*(s)$  stands for the  $p$  different scaled non-nominal systems, one for each operating point, where the controller is required to work properly.

2. Design of weighting functions

Once the multiplicative uncertainty has been estimated, function  $W_T(s)$  in such a way that it must be stable, minimum phase, with high gain at high frequencies, and with module greater than the module of the uncertainty previously computed for each non-nominal model and frequency, that is,

$$|W_T(j\omega)| \geq |E_{oi}(j\omega)| \quad \forall \omega, \forall p$$

For this application, the following design is carried out

$$W_T(s) = \frac{0.52(0.66s + 1)}{0.1s + 1}$$

which fulfills the above constraints, as shown in figure 8.

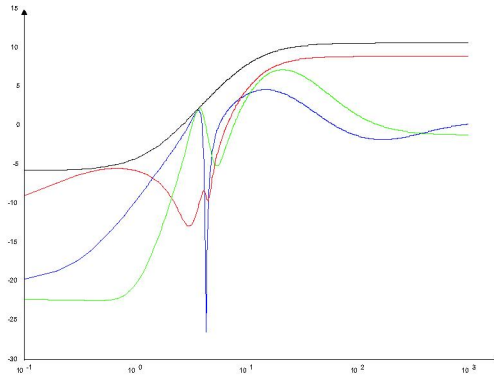


**Figure 8. Function  $W_T(s)$  as an upper bound of the estimated multiplicative uncertainty**

Regarding to the weighting function  $W_S(s)$ , its design is proposed as following expression:

$$W_S(s) = \frac{\alpha s + 10^{(\kappa-1)}\omega_T}{s + \beta 10^{(\kappa-1)}\omega_T}$$

where  $\omega_T \simeq 2.8 \text{ rad/s}$  is the crossover frequency of the transfer function  $W_T(s)$ . The following values are proposed for the parameters:  $\alpha \simeq 0.5$ ,  $\beta \simeq 10^{-4}$ , and  $\kappa$  initially equal to 0. The final form of  $W_S(s)$  is obtained by adjusting the value of  $\kappa$  under instructions of the following rule of thumb: *as the value of  $\kappa$  increases, a faster (although more oscillatory) response is attained*.

Finally, the weighting function  $W_{KS}(s)$  is chosen as the identity in order to avoid numerical problems [3].

### 3. Buliding up the generalized plant and obtaining the controller

As a final step, the generalized plant  $P(s)$  must be built up using the nominal model and weighting functions previously designed (see figure 7). Taking as starting data the generalized plant, the controller may be attained by means of some synthesis method implemented in some software package, such as [3], and [2].

At this point it is important to remember that the controller has been computed by means of a scaled model. Thereby, an inverse-scale process must be performed on the controller before implementing it in the real plant.

The tuning procedure for the parameter  $\kappa$  has been performed by direct inspection of the experimental response. Experimental results obtained with this control strategy

are shown in figure 9. It can be seen some tracking improvements in relation to the ones of the PID controller, while poor results are achieved in disturbance rejection experiments. The time response becomes too oscillatory, and with a great amplitude. This may be explained keeping in mind that this is model-based controller, which tries to cancel the system dynamics. In this way, it must be remembered that the system has a dominant and very oscillatory mode. These poles vary depending on the operating point. Therefore, the oscillations may be caused by an imperfect cancellation of these poles.

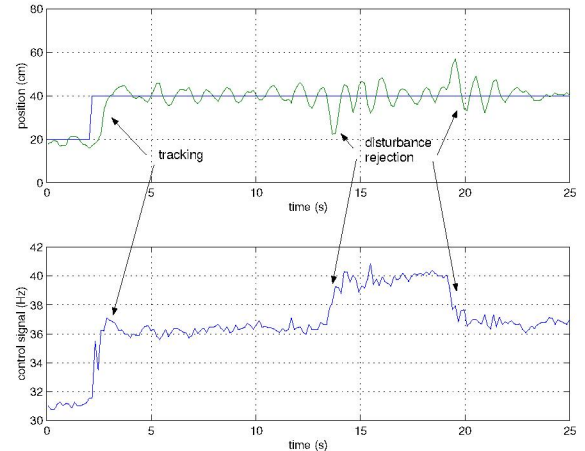


**Figure 9. Experimental results with the  $H_\infty$  controller**

### 3.3 Fuzzy control

The third control strategy implemented is based on fuzzy logic [9, 5]. In particular, a *pseudo-linear direct control* has been designed, which is, in some sense, similar to a PI controller [4]. Figure 10 shows the structure of a general fuzzy controller.

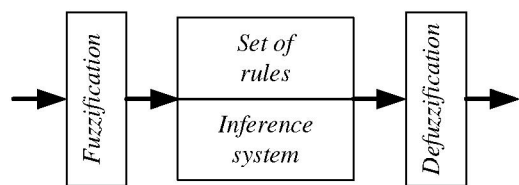


**Figure 10. Structure of a fuzzy controller**

In the case of a direct controller, the inputs only depend on the error, while the output is oriented towards the manipulated variable. In this work, an incremental controller has been synthesized, whose inputs are the error and its derivative, weighted by the parameters  $K_1$  and  $K_2$  respectively (see figure 11). The output is the derivative of the manipulated variable, which is weighted by the parameter  $K_3$ .

On the one hand, two triangular membership functions for each input are established, with their peak values at -1 and 1 respectively. On the other hand, three singletons

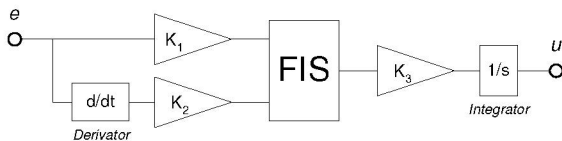


**Figure 11. Structure of an incremental fuzzy controller**

are employed for each output, whose values are -1, 0, and 1 respectively. The following names are adopted for the inputs: *positive* and *negative*; and the following for the outputs: *negative*, *zero*, and *positive*.

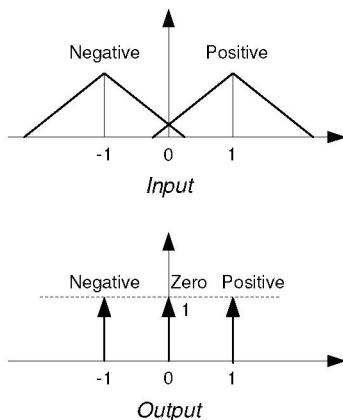


**Figure 12. Input and output membership functions**

The base for this controller consists of the following four rules:

- If  $e$  is *positive* and  $de$  is *positive* then  $du$  is *positive*
- If  $e$  is *positive* and  $de$  is *negative* then  $du$  is *zero*
- If  $e$  is *negative* and  $de$  is *positive* then  $du$  is *zero*
- If  $e$  is *negative* and  $de$  is *negative* then  $du$  is *negative*

Despite of the resultant fuzzy controller is nonlinear, there are some similarities among the parameters of these controller and the ones of a PID. In fact, once the parameter  $K_1$  has been adjusted, the parameter  $K_2$  plays the role of the integral time, whilst the parameter  $K_3$  is similar to the proportional gain.

The following rule is employed the defuzzification process:

$$u = \frac{\sum_{i=1}^n \mu_i \cdot S_i}{\sum_{i=1}^n \mu_i}$$

where  $n$  is the number of singletons (in this case, three: -1, 0, and 1) and  $\mu_i$  is the membership grade associated to the  $i$  singleton.

Experimental results attained with this control strategy are shown in figure 13. In this case, the speed of the time

response is similar to the ones attained by the previous controllers, but the amplitude of the oscillations decreases a lot, at least in disturbance rejection experiments.

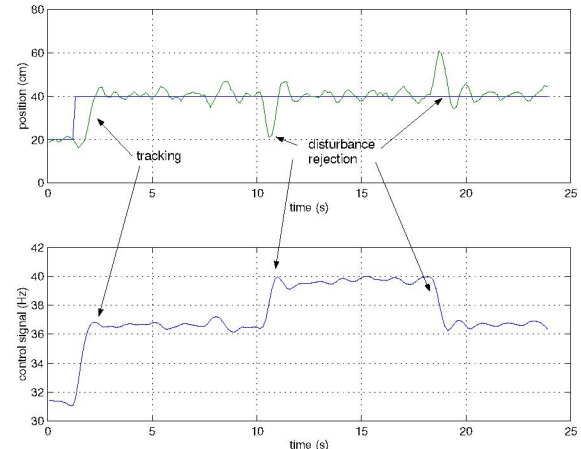


**Figure 13. Experimental results with the fuzzy controller**

### 3.4 Comparison of results

In order to compare the results attained by the control strategies, the ITAE index of the time responses are exposed in table 1.

	Tracking	Disturbance rejection
PID	19.42	10.88
$H_\infty$	17.54	16.12
Fuzzy	18.66	9.72

**Table 1. ITAE index for each controller**

It can been observed that the implemented PID controller supplies a good trade-off between tracking and disturbance rejection problems. The  $H_\infty$  controller is able to improve the tacking performance, but at the expense of a poor performance in the disturbance rejection. Finally, it can been noted that the implemented fuzzy control law slightly improves the performance supplied by the PID controller in both cases.

It is worth pointing out that both PID and fuzzy controller provide smooth control signals (see figures 6 and 13). However, the control signal generated by the  $H_\infty$  controller has a significant high frequency component (see figure 9). This fact should be kept in mind in order to avoid the damage of the system.

## 4 Conclusions

A lab plant, which consists of industrial components, has been used to study suitable control strategies for the position control of pneumatic levitation systems. A brief

modelling study has been performed, and linearized systems around several operating points has been obtained from analyzing input-output data.

Three control strategies has been implemented, and experimental results for tracking and disturbance rejection have been presented. The first controller has been a classical PID, which has provided a good trade-off between tracking and disturbance rejection.

A pseudo-linear direct control based on fuzzy logic has been also tested. Despite of few rules have been designed, with triangular membership functions for the inputs and three singletons for the output, this controller has slightly improved the performance attained with the PID.

Finally, a model-based  $H_\infty$  controller has been also tried out. Although better behavior has been achieved for tracking experiments, this controller has provided a poor performance for disturbance rejection. This fact may be explained taking into account the uncertainty of the system dominant mode, which is too oscillatory.

## Acknowledgments

The authors would like to acknowledge MCYT and FEDER for funding this work under grants DPI2003-00429 and DPI2004-06419. Likewise, the authors appreciate the support of the DMASTEC organization.

## References

- [1] Algarín, D. *Reconocimiento de objetos mediante visión artificial* (in Spanish). Proyecto Integrado, Centro Tecnológico ALTAIR, 2002. In Spanish.
- [2] Balas, G., Doyle, J., Glover, K., Packard, A., Smith, R.  $\mu$ -*Analisis and Synthesis Toolbox User's Guide*. The MathWorks Inc., Natick, Mass, second edition, 1995.
- [3] Chiang, R., Safonov, M. *Robust Control Toolbox User's Guide*. The MathWorks Inc., Natick, second edition, 1998.
- [4] Jantzen, J. *Tuning of Fuzzy PID Controllers*. Technical University of Denmark. Departament of Automation, Bldg 326, DK-2800 Lyngby., second edition, 1998. Tech. Report no 98-H 871.
- [5] Leondes, C.T. *Fuzzy Theory Systems. Techniques and Applications*. Academic Press, 1999.
- [6] Ljung, L. *System Identification Toolbox*. The Math Works, Inc., 1995.
- [7] Ortega, M.G., Rubio, F.R. "Systematic Design of Weighting Matrices for  $H_\infty$  mixed Sensitivity Problem". *Journal of Process Control*, 14(1):89–98, 2004.
- [8] Reed, J. *Biscuit Levitation by airjets*. Biennial Report 1998-2000, Silsoe Research Institute, New York, 2000.
- [9] Rubio, F.R., Berenguel, M., Camacho, E.F. Fuzzy Logic Control of a Solar Power Plant. *IEEE Trans. on Fuzzy Systems*, 3(4), 1995.
- [10] Skogestad, S., Postlethwaite, I. *Multivariable Feedback Control. Analysis and Design*. Jonh Wiley & Sons, New York, 1996.